Model of radiative heat transfer in heterogeneous multiphase media

A. V. Gusarov*
ENISE, 58 rue Jean Parot, 42023 Saint-Etienne, France
(Received 3 December 2009; revised manuscript received 22 January 2010; published 12 February 2010)

The radiative contribution to the thermal conductivity of composite media is analyzed by the Chapman-Enskog expansion of a multiphase radiation transfer model. The radiative thermal conductivity obtained generalizes the Rosseland diffusion approximation and is presented as function of the phase composition of the medium, the specific surface of the phase boundaries, and the spectral optical properties of the phases, namely, the refractive index and the absorption coefficient. It is applicable in the domain of parameters where the scattering of thermal radiation can be considered in the approximation of geometrical optics. The obtained results are compared with those derived by the Mie theory for dilute dispersions. A considerable discrepancy is revealed only when the diameter of the dispersed scatterers becomes inferior to the wavelength. The results are also compared with experiments on high-temperature thermal conductivity in packed beds where the Mie theory cannot be applied because of dependent scattering of thermal radiation. The experimental validation covers the range of particle sizes from 45 μm to 11 mm and the temperature interval from ~300 to ~1200 K. The relation between the theory and the experiments is classified from satisfactory agreement in the best case to consistency in the worst case.

DOI: 10.1103/PhysRevB.81.064202 PACS number(s): 44.35.+c, 44.30.+v

I. INTRODUCTION

Heat transfer in heterogeneous materials is of continuous interest for more than hundred years starting by the theoretical study of the Laplace equation for dispersed media by Maxwell.[1] The history of this subject is covered in monographs such as[2] and some research papers.[3,4] Numerous recent publications[5–9] are inspired by unceasing progress in the technology of materials proposing more and more complex composite structures. The principal directions of the current theoretical studies are general methods for description and reconstruction of heterogeneous structures,[10] multiscale modeling,[11] and multiphysics applications considering, for example, the contribution of molecular heat transfer in the gas phase[4] or the phonon transport in the ballistic regime.[12]

The radiative heat transfer perceived as multiple absorption and re-emission of the thermal radiation can be the principal heat transfer mechanism at certain conditions or it can act in parallel to other physical transport processes of different nature. In the both cases the radiative thermal conductivity can be introduced as the ratio of the radiative contribution to the heat flow to the temperature gradient. The radiative heat transfer in heterogeneous media is traditionally important for the high-temperature[13–15] and geophysical[16] domains and finds various other applications.[17,18] In porous materials the radiative thermal conductivity can be estimated by approaches for radiative transfer between opaque bodies for a given morphology of pores.[19,20] Rosseland[21] was first who found a relation between the radiative thermal conductivity and the general radiative properties as the absorption coefficient. Various expansions of the radiation transfer equation (RTE) in an optically thick domain[22–24] result in similar relations, which is recognized to be the most general way to estimate the radiative thermal conductivity.

Radiation transfer in dilute dispersions is rigorously described by the RTE with the coefficients referred to as the radiative properties estimated from radiation scattering by individual particles.[25] The subject of the present study is not dilute but dense dispersed media or, generally, multiphase media with comparable volume fractions of different phases. One has never proven that radiation transfer in a dense dispersed system can be described by a RTE because of so-called dependent scattering, i.e., influence of neighbor particles. Even if the model of RTE is accepted for a multiphase medium, the Mie theory of scattering[25] is no more satisfactory to estimate the radiative properties, and additional efforts are required for theoretical or experimental identification thereof.[26]

Currently, the so-called multiphase RTE (MRTE) is considered to be a promising theoretical model for multiphase media where each phase is characterized by its own average radiation intensity, thus producing a system of coupled integrodifferential equations, each of them similar to a single RTE. The MRTE was first derived for a medium with a single absolutely transparent phase and the other phases being completely opaque.[27,28] However, this case is, obviously, reduced to a single RTE and is interesting only as a method to estimate the dependent radiative properties. The general case of MRTE for arbitrary optical properties of phases is discussed in recent publications.[29–31] The formal MRTE model is more general than the conventional RTE because the proper choice of parameters of MRTE reduces it to a single RTE in the case where the RTE is proved to be rigorous, for example, in dilute dispersions. On the other hand, the examples of the mixture of a transparent and an opaque phases with comparable volume fractions and the mixture of two transparent phases with considerably different refractive indices and comparable volume fractions[30] show that characterization of radiation by a single intensity accepted in the RTE is insufficient and the two partial intensities for each phase in the framework of MRTE allow a more precise characterization.

Our previous relevant publications concern conductive heat transfer controlled by necks of condensed phase be-

tween particles in powder and packed beds,[32] heat transfer controlled by molecular transport through the gas phase in powder and packed beds,[3] along with coupling of the two above mechanisms.[4] Radiation transfer in multiphase media is considered in the cases of one transparent phase and other opaque phases[28] and two phases with arbitrary optical properties.[30] The present paper reduces the developed models for radiation transfer to Fourier's law by the Chapman-Enskog analysis in case of optically thick media. The resulting radiative thermal conductivity complements previous models of heat transfer.[3,4,32]

The objective is obtaining a theoretical expression for the radiative thermal conductivity as function of phase composition, optical properties of phases, and morphological parameters of the medium. The study is based on the MRTE model described in Sec. II, which was proposed and validated in Ref. 30. The radiative properties of this model are estimated in the approximation of geometrical optics. The radiative thermal conductivity itself is obtained from the MRTE by the Chapman-Enskog expansion in Sec. III. The result is analyzed in Sec. IV and compared with known theoretical models in Sec. V and experimental data in Sec. VI.

II. MULTIPHASE MODEL

Radiation transfer in a multiphase medium can be described by a system of radiation transfer equations for partial spectral radiation intensities $I_{\nu\gamma}$ with index ν indicating the photon frequency and γ the number of phase. The partial intensity $I_{\nu\gamma}$ is defined as the average of the local radiation intensity over phase γ within a reference domain of the medium.[30] Assuming that sequential scattering events at phase boundaries are independent, the geometrical optics laws give the following radiation transfer equations for a two-phase statistically isotropic heterogeneous medium with $\gamma=0,1$ (Ref. 30):

$$\begin{aligned}\mathbf{\Omega}\nabla I_{\nu 0} &= \alpha_0 n_0^2 B_\nu - \left(\alpha_0 + \frac{\mathcal{A}_{01}}{4f_0}\right) I_{\nu 0} \\ &+ \frac{\mathcal{A}_{01}\rho_{01}}{4f_0}\frac{1}{4\pi}\int_{4\pi} I_{\nu 0}(\mathbf{\Omega}')\mathcal{R}_{01}(\mathbf{\Omega}',\mathbf{\Omega})d\mathbf{\Omega}' \\ &+ \frac{\mathcal{A}_{01}(1-\rho_{10})}{4f_0}\frac{1}{4\pi}\int_{4\pi} I_{\nu 1}(\mathbf{\Omega}')\mathcal{T}_{10}(\mathbf{\Omega}',\mathbf{\Omega})d\mathbf{\Omega}',\end{aligned} \tag{1}$$

$$\begin{aligned}\mathbf{\Omega}\nabla I_{\nu 1} &= \alpha_1 n_1^2 B_\nu - \left(\alpha_1 + \frac{\mathcal{A}_{01}}{4f_1}\right) I_{\nu 1} \\ &+ \frac{\mathcal{A}_{01}\rho_{10}}{4f_1}\frac{1}{4\pi}\int_{4\pi} I_{\nu 1}(\mathbf{\Omega}')\mathcal{R}_{10}(\mathbf{\Omega}',\mathbf{\Omega})d\mathbf{\Omega}' \\ &+ \frac{\mathcal{A}_{01}(1-\rho_{01})}{4f_1}\frac{1}{4\pi}\int_{4\pi} I_{\nu 0}(\mathbf{\Omega}')\mathcal{T}_{01}(\mathbf{\Omega}',\mathbf{\Omega})d\mathbf{\Omega}',\end{aligned} \tag{2}$$

where $\mathbf{\Omega}$ is the unit vector of direction, α_γ the absorption coefficient in phase γ, n_γ the refractive index, f_γ the volume fraction of phase γ, $\mathcal{A}_{01}$ the specific surface of 0–1 phase boundaries per unit volume, $\rho_{\gamma\delta}$ the hemispherical reflectivity for the incidence from phase γ to phase δ,

$$B_\nu d\nu = \frac{2h\nu^3 d\nu}{c^2(e^{h\nu/kT}-1)}, \tag{3}$$

the blackbody radiation in vacuum[33] with h Planck's constant, c the speed of light in vacuum, k the Boltzmann constant, and T the temperature, and the scattering phase functions,[30]

$$\mathcal{R}_{\gamma\delta}(\mathbf{\Omega}',\mathbf{\Omega}) = \frac{\rho'_{\gamma\delta}(\chi)}{\rho_{\gamma\delta}}, \tag{4}$$

$$\mathcal{T}_{10}(\mathbf{\Omega}',\mathbf{\Omega}) = \mathcal{T}_{01}(\mathbf{\Omega}',\mathbf{\Omega}) = 2\frac{1-\rho_{01}{}'(\chi_0)}{1-\rho_{01}}\frac{d\cos^2\chi_0}{d\cos(\chi_0-\chi_1)}, \tag{5}$$

with $\rho_{\gamma\delta}{}'(\chi)$ as the directional reflectivity for the incidence from phase γ to phase δ, $\chi=(\pi-\psi)/2$ as the angle of incidence corresponding to specular reflection at the scattering angle ψ, $\cos\psi=(\mathbf{\Omega}',\mathbf{\Omega})$, χ_0 and χ_1 are the angles of incidence and refraction, respectively, corresponding to refraction at the scattering angle ψ, which can be found from Snell's refraction law $n_0\sin\chi_0=n_1\sin\chi_1$ and the scattering relation[30] $\psi=|\chi_0-\chi_1|$.

Fresnel's equation gives the directional reflectivity of unpolarized radiation by materials with small extinction index,[33]

$$\rho_{01}{}'(\chi_0) = \frac{1}{2}\frac{\sin^2(\chi_1-\chi_0)}{\sin^2(\chi_1+\chi_0)}\left[1+\frac{\cos^2(\chi_1+\chi_0)}{\cos^2(\chi_1-\chi_0)}\right]. \tag{6}$$

The hemispherical reflectivity is the weighted average over the incidence angle χ,

$$\rho_{\gamma\delta} = 2\int_0^1 \rho_{\gamma\delta}{}'(\chi)\cos\chi d\cos\chi. \tag{7}$$

The following reciprocity relations are useful for the directional reflectivity:

$$\rho_{01}{}'(\chi_0) = \rho_{10}{}'(\chi_1), \tag{8}$$

and for the hemispherical reflectivity,

$$n_0^2(1-\rho_{01}) = n_1^2(1-\rho_{10}). \tag{9}$$

The partial radiation intensities obtained from Eqs. (1) and (2) give the integral homogenized intensity defined as the average of the local intensity over the reference domain,[30]

$$I_\nu = f_0 I_{\nu 0} + f_1 I_{\nu 1}. \tag{10}$$

The homogenized spectral heat flux is defined as a moment of I_ν,[33]

$$\mathbf{q}_\nu = \int_{4\pi} I_\nu(\mathbf{\Omega})\mathbf{\Omega} d\mathbf{\Omega}. \tag{11}$$

Finally, the total heat flux is

$$\mathbf{q} = \int_0^\infty \mathbf{q}_\nu d\nu. \tag{12}$$

III. CHAPMAN-ENSKOG ANALYSIS

Consider a slightly nonuniform state of the medium characterized by the spatial distribution of its local temperature T. According to the Chapman-Enskog method,[34] the solution of the system of integrodifferential Eqs. (1) and (2) can be expanded in series with the smallness parameter proportional to $|\nabla T|$,

$$I_{\nu\gamma} = I_{\nu\gamma}^{(0)} + I_{\nu\gamma}^{(1)} + I_{\nu\gamma}^{(2)} + \cdots, \tag{13}$$

where the zero-order term corresponds to the thermodynamic equilibrium at temperature T,

$$I_{\nu\gamma}^{(0)} = n_\gamma^2 B_\nu(T), \tag{14}$$

and the higher-order terms can be found from the infinite set of integral equations,

$$\begin{aligned}\mathbf{\Omega}\nabla I_{\nu 0}^{(j)} = &-\left(\alpha_0 + \frac{\mathcal{A}_{01}}{4f_0}\right) I_{\nu 0}^{(j+1)} \\ &+ \frac{\mathcal{A}_{01}\rho_{01}}{4f_0}\frac{1}{4\pi}\int_{4\pi} I_{\nu 0}^{(j+1)}(\mathbf{\Omega}')\mathcal{R}_{01}(\mathbf{\Omega}',\mathbf{\Omega})d\mathbf{\Omega}' \\ &+ \frac{\mathcal{A}_{01}(1-\rho_{10})}{4f_0}\frac{1}{4\pi}\int_{4\pi} I_{\nu 1}^{(j+1)}(\mathbf{\Omega}')\mathcal{T}_{10}(\mathbf{\Omega}',\mathbf{\Omega})d\mathbf{\Omega}',\end{aligned} \tag{15}$$

$$\begin{aligned}\mathbf{\Omega}\nabla I_{\nu 1}^{(j)} = &-\left(\alpha_1 + \frac{\mathcal{A}_{01}}{4f_1}\right) I_{\nu 1}^{(j+1)} \\ &+ \frac{\mathcal{A}_{01}\rho_{10}}{4f_1}\frac{1}{4\pi}\int_{4\pi} I_{\nu 1}^{(j+1)}(\mathbf{\Omega}')\mathcal{R}_{10}(\mathbf{\Omega}',\mathbf{\Omega})d\mathbf{\Omega}' \\ &+ \frac{\mathcal{A}_{01}(1-\rho_{01})}{4f_1}\frac{1}{4\pi}\int_{4\pi} I_{\nu 0}^{(j+1)}(\mathbf{\Omega}')\mathcal{T}_{01}(\mathbf{\Omega}',\mathbf{\Omega})d\mathbf{\Omega}',\end{aligned} \tag{16}$$

for $j=0,1,2,\ldots$.

In the lowest order $j=0$, the left-hand sides of Eqs. (15) and (16) are proportional to a projection of the unit vector of direction $\mathbf{\Omega}$,

$$\mathbf{\Omega}\nabla I_{\nu\gamma}^{(0)} = n_\gamma^2 \frac{dB_\nu}{dT}\mathbf{\Omega}\nabla T. \tag{17}$$

On the other hand, function $\mathbf{\Omega}$ is the eigenfunction of the scattering operators in case of an isotropic medium,

$$\begin{aligned}\frac{1}{4\pi}\int_{4\pi}\mathcal{R}_{\gamma\delta}(\psi)\mathbf{\Omega}'d\mathbf{\Omega}' = R_{\gamma\delta}\mathbf{\Omega}, \quad \frac{1}{4\pi}\int_{4\pi}\mathcal{T}_{\gamma\delta}(\psi)\mathbf{\Omega}'d\mathbf{\Omega}' \\ = T_{\gamma\delta}\mathbf{\Omega},\end{aligned} \tag{18}$$

where $\psi=\arccos(\mathbf{\Omega}',\mathbf{\Omega})$ is the scattering angle and $R_{\gamma\delta}$ and $T_{\gamma\delta}$ are the corresponding eigenvalues. Therefore, the first-order term in expansion (13) is sought as

$$I_{\nu\gamma}^{(1)} = (\mathbf{i}_\gamma,\mathbf{\Omega}), \tag{19}$$

with the unknown vector $\mathbf{i}_\gamma$ independent of angle $\mathbf{\Omega}$. Substituting Eq. (19) in Eqs. (15) and (16) at $j=0$ reduces them to a system of linear algebraic equation relative $\mathbf{i}_\gamma$. Finally, the first-order term of the Chapman-Enskog expansion is found as

$$I_{\nu 0}^{(1)} = -\frac{n_0^2 f_0 a_{11} + n_0 n_1 f_1 a_{01}}{a_{00}a_{11} - a_{01}^2}\frac{4}{\mathcal{A}_{01}}\frac{dB_\nu}{dT}\mathbf{\Omega}\nabla T, \tag{20}$$

$$I_{\nu 1}^{(1)} = -\frac{n_1^2 f_1 a_{00} + n_0 n_1 f_0 a_{01}}{a_{00}a_{11} - a_{01}^2}\frac{4}{\mathcal{A}_{01}}\frac{dB_\nu}{dT}\mathbf{\Omega}\nabla T, \tag{21}$$

with

$$a_{00} = 1 + g_0 - \rho_{01}R_{01}, \tag{22}$$

$$a_{01} = T_{01}\sqrt{(1-\rho_{01})(1-\rho_{10})}, \tag{23}$$

$$a_{11} = 1 + g_1 - \rho_{10}R_{10}, \tag{24}$$

$$g_\gamma = \frac{4f_\gamma\alpha_\gamma}{\mathcal{A}_{01}}. \tag{25}$$

Successive application of Eqs. (10)–(12) to solutions (20) and (21) results in the radiative heat flux presented as the Fourier's law with the accuracy up to the first Chapman-Enskog term,

$$\mathbf{q} = -\Lambda\nabla T, \tag{26}$$

with the radiative thermal conductivity

$$\Lambda = \frac{64\sigma T^3}{3\mathcal{A}_{01}}\int_0^\infty HRdx, \tag{27}$$

where

$$\sigma = \frac{2}{15}\frac{\pi^5 k^4}{c^2 h^3}, \tag{28}$$

is the Stefan-Boltzmann constant,

$$x = \frac{h\nu}{kT}, \tag{29}$$

the reduced frequency,

$$H(x) = \frac{n_0^2 f_0^2 a_{11} + 2n_0 n_1 f_0 f_1 a_{01} + n_1^2 f_1^2 a_{00}}{a_{00}a_{11} - a_{01}^2}, \tag{30}$$

the spectral structure factor, and

$$R = \frac{15}{4\pi^4}\frac{x^4 e^x}{(e^x-1)^2}, \tag{31}$$

Rosseland's weight function.[21] Equation (27) generalizes Rosseland's diffusion approach[21] to the multiphase medium. It takes into account the spectral optical properties of the phases through the structure factor H, Eq. (30), which depends on the phase volumetric fractions f_γ, their refractive indices n_γ and absorption coefficients α_γ, the hemispherical reflectivities $\rho_{\gamma\delta}$ of the interfaces, and the eigenvalues $R_{\gamma\delta}$ and $T_{\gamma\delta}$ of the scattering integrals. The above results are applicable in the domain of parameters where the scattering of the thermal radiation can be considered in the approximation of the geometrical optics because the coefficients of the base model of radiation transfer[30] are obtained in this approximation.

Eigenvalues of the scattering integrals

The eigenvalues of the scattering integrals corresponding to the eigenfunction $\mathbf{\Omega}$ are defined by Eq. (18). The definitions of scattering phase functions (4) and (5) through the directional reflectivity $\rho_{\gamma\delta}{}'(\chi)$ useful for geometrical optics reduce calculation of the eigenvalues to the following integrals:

$$\rho_{\gamma\delta}(1-R_{\gamma\delta}) = 4\int_0^1 \rho_{\gamma\delta}{}'(\chi)\cos^3\chi d\cos\chi, \tag{32}$$

$$(1-\rho_{01})T_{01} = 2\int_0^1 [1-\rho_{01}{}'(\chi_0)]\cos(\chi_0-\chi_1)\cos\chi_0 d\cos\chi_0, \tag{33}$$

where the incidence χ_0 and the refraction χ_1 angles are related by Snell's law. The optical reciprocity, Eq. (8), results in the following reciprocity relations for the eigenvalues:

$$n_0^4[1-\rho_{01}(1+R_{01})] = n_1^4[1-\rho_{10}(1+R_{10})], \tag{34}$$

$$T_{01} = T_{10}. \tag{35}$$

Equation (34) should be applied along with the reciprocity for the hemispherical reflectivities given by Eq. (9). Integrals (32) and (33) are numerically calculated for Fresnel's directional reflectivity, Eq. (6), and plotted in Fig. 1 along with the hemispherical reflectivities [Eq. (7)].

IV. MODELS OF MULTIPHASE MEDIA

The key issue of the above theory is estimation of the structure factor H given by Eq. (30), which depends on the morphological characteristics of the multiphase medium and the spectral optical properties of the phases. The complete set of these parameters is rarely available from experiments. Sometimes the inverse problem of identifying the missing parameters can be posed. For these purposes, simplified models and limiting cases with reduced number of parameters are useful.

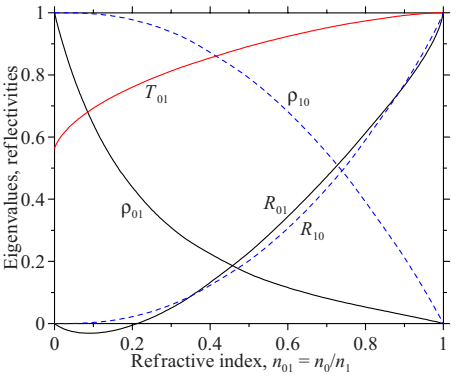

FIG. 1. (Color online) Eigenvalues R_{01}, R_{10}, and $T_{01}=T_{10}$ of the scattering integrals and hemispherical reflectivities ρ_{01} and ρ_{10} versus the ratio of the refractive indices $n_{01}=n_0/n_1$ for Fresnel's reflection law.

A. Dilute dispersed systems

Let phase 1 with negligible volume fraction be dispersed in matrix 0. The multiphase model of radiation transfer [Eqs. (1) and (2)] is shown[30] to reduce to single RTE in this case. The Chapman-Enskog analysis can be applied to the reduced equation. The same result is expected in the limit $f_1 \to 0$ applied to general structure factor (30),

$$H = \frac{n_0^2 a_{11}}{a_{00}a_{11}-a_{01}^2}. \tag{36}$$

Radiative thermal conductivity (27) is reduced to the conventional for Rosseland's approximation form,[33]

$$\Lambda = \frac{16\sigma T^3}{3}\int_0^\infty \frac{n_0^2 R dx}{\beta_{\rm tr}}, \tag{37}$$

where the transport extinction coefficient is evaluated as

$$\beta_{\rm tr} = (a_{00} - a_{01}^2/a_{11})\frac{\mathcal{A}_{01}}{4}. \tag{38}$$

1. Isotropic dispersed scatterers

The well-known example of an isotropic scatterer is a specularly reflecting opaque ($\alpha_1 \to \infty$) sphere with the directional reflectivity of its surface independent of the incidence.[33] In this case the multiphase model is reduced to an RTE with the scattering phase function[30]

$$\mathcal{R}_{01} = 1. \tag{39}$$

According to definition (18), the isotropic scattering corresponds to the eigenvalue

$$R_{01} = 0. \tag{40}$$

Thus, the case of dilute dispersed isotropic scatterers is given by the limit of Eq. (38) at $\alpha_1 \to \infty$ and eigenvalue (40),

$$\beta_{\rm tr}^{\rm isotropic} = \frac{\mathcal{A}_{01}}{4} + \alpha_0, \tag{41}$$

with the first term in the right-hand side equal to the scattering coefficient.[30] In the considered case, the transport extinc-

tion coefficient β_{tr} is the sum of the scattering and absorption coefficients referred to as the extinction coefficient β.

Equation (41) is independent of the physics of scattering and is applicable to an arbitrary absorbing isotropically scattering medium where radiation transfer is described by an RTE with scattering phase function (39). For example, the isotropic scattering is produced not only by specularly reflecting spheres but also by arbitrary convex randomly oriented particles with constant directional reflectivity.[35] This model is satisfactory for scatterers-metallic particles with the size well above the wavelength to assure reflection according to the laws of geometrical optics.[36]

2. Scattering by opaque diffusely reflecting particles

In the limit of opaque phase 1, the radiation is excluded from this phase so that the only significant component of the phase function matrix is $\mathcal{R}_{01}$. Transport extinction coefficient (38) becomes

$$\beta_{tr} = \frac{\mathcal{A}_{01}}{4}(1 - \rho_{01}R_{01}) + \alpha_0. \tag{42}$$

Indeed, it contains only the scattering parameters related to $\mathcal{R}_{01}$, namely, the hemispherical reflectivity ρ_{01} and the eigenvalue R_{01}. Diffusely reflecting spherical[33] as well as randomly oriented convex[35] particles scatter with the following phase function:

$$\mathcal{R}_{01}(\psi) = \frac{8}{3\pi}(\sin\psi - \psi\cos\psi). \tag{43}$$

An example of diffusely reflecting particles is given by agglomerates of nanoparticles.[36] Function (43) monotonously increases with the scattering angle ψ in the range from 0 to π, which signifies preferentially backward scattering. Therefore, reducing the radiative heat transfer relative isotropic scattering is expected. Indeed, the eigenvalue obtained from Eq. (18) as

$$R_{01} = \frac{1}{2}\int_{-1}^{1}\mathcal{R}_{01}(\psi)\cos\psi d\cos\psi = -\frac{4}{9}. \tag{44}$$

is negative so that increasing the diffuse reflectivity ρ_{01} increases transport extinction coefficient (42). The maximum "thermal insulating" effect is attained for a transparent matrix with $\alpha_0=0$ at $\rho_{01}=1$. As follows from Eqs. (42) and (44), the transport extinction coefficient is increased by a factor of 13/9 at these conditions and, hence, the heat flux is reduced by this factor.

3. Opaque dielectric particles

An opposite example of preferentially forward scattering is given by dielectric particles[33] where radiative heat transfer is expected to be enhanced relative the case of isotropic scattering. The enhancement factor can be introduced as the ratio of the corresponding structure factors or transport scattering coefficients. Thus, for opaque particles in transparent matrix Eqs. (41) and (42) result in

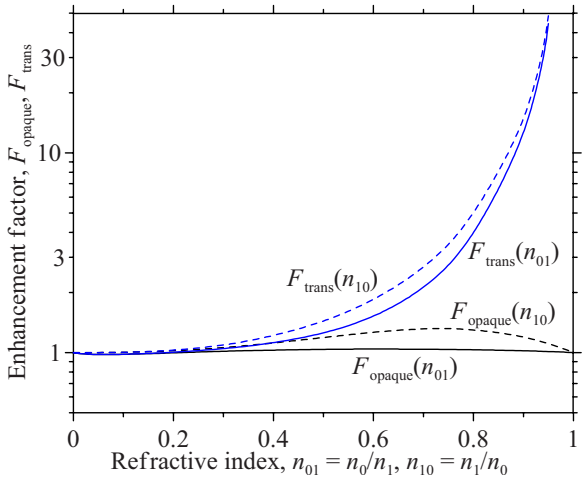

FIG. 2. (Color online) Radiative heat transfer enhancement factors for dilute dispersions of opaque, F_{opaque}, and transparent, F_{trans}, dielectric particles with small extinction index (phase 1) in transparent matrix (phase 0) versus the ratio of refractive indices, $n_{01}=1/n_{10}$: denser particles in lighter matrix (full curves) and lighter particles in denser matrix (broken curves).

$$F_{opaque} = \frac{H_{opaque}}{H_{isotropic}} = \frac{\beta_{tr}^{isotropic}}{\beta_{tr}^{opaque}} = \frac{1}{1 - \rho_{01}R_{01}}. \tag{45}$$

The lower full and broken curves in Fig. 2 show this enhancement factor for dielectrics with small extinction index reflecting according to Eq. (6) where reflectivity ρ_{01} and eigenvalue R_{01} correspond to Fig. 1. The effect of the forward scattering by opaque dielectric particles is small because ρ_{01} tends to zero where R_{01} tends to unity and vice versa.

4. Transparent dielectric particles

The scattering coefficient and phase function by transparent particles of a specified shape can be calculated by ray optics. Such a rigorous method takes into account sequential internal reflections.[33] The Chapman-Enskog method can be applied in this case. The multiphase model neglecting correlation between internal reflections gives an approximate but satisfactory description[30] independent of the particle shape. An approximate structure factor for dilute dispersion of transparent particles can be obtained in the framework of the multiphase model from Eq. (36). Thus, the enhancement factor for transparent particles in transparent matrix is

$$F_{trans} = \frac{H_{trans}}{H_{isotropic}} = \frac{\beta_{tr}^{isotropic}}{\beta_{tr}^{trans}} = \frac{1 - \rho_{10}R_{10}}{(1 - \rho_{10}R_{10})(1 - \rho_{01}R_{01}) - (1 - \rho_{01})(1 - \rho_{10})T_{01}^2}, \tag{46}$$

where the reflectivities and the eigenvalues are given in Fig. 1 The upper full and broken curves in Fig. 2 show this factor. It tends to infinity when the ratio of refractive indices tends to unity because phase boundaries vanish in this limit.

B. Dense dispersed systems

If the volume fraction of the dispersed phase f_1 is comparable with that of the matrix f_0, Eq. (36) obtained for dilute dispersions is not valid and general Eq. (30) for the structure factor should be applied. Consider the difference between dilute and dense dispersions on the example of opaque dispersed phase 1. In this case Eq. (37) is modified as

$$\Lambda = \frac{16 f_0 \sigma T^3}{3} \int_0^\infty \frac{n_0^2 R dx}{\beta_{\rm tr}}, \tag{47}$$

with

$$\beta_{\rm tr} = \frac{\mathcal{A}_{01}}{4 f_0}(1 - \rho_{01} R_{01}) + \alpha_0. \tag{48}$$

These equations give right dilute limit, Eqs. (37) and (42), and predict vanishing of the radiative heat transfer at very high fraction of the dispersed phase $f_1 = 1 - f_0 \to 1$ when radiation is blocked by the opaque phase. The factor of f_0 in Eq. (47) signifies that only the transparent phase contributes to the heat transfer. The factor of $1/f_0$ in the first term of the right-hand side of Eq. (48) is the so-called scaling factor introduced to take into account the exclusion of radiation from the opaque phase.[30] There are no restrictions to apply Eq. (48) at high fractions of the opaque phase, when it becomes not dispersed but continuous. However, matrix phase 0, where radiation is transferred, is supposed to be still continuous.

C. Models of spectral properties

Estimation of spectral integrals, for example, in Eqs. (27), (37), and (47), requires the detailed spectral optical properties of the phases, which are not always available. Therefore, simplified spectral models are useful.

1. Gray media

If the optical properties of the phases are independent of the radiation frequency (wavelength), the structure factor H can be factor out of integral (27),

$$\Lambda = \frac{64 \sigma T^3}{3 \mathcal{A}_{01}} H, \tag{49}$$

where the integral of the Rosseland function R gives unity. General expression (30) as well as any of the above structure models can be used to estimate the structure factor H.

2. Mixture of a transparent and a semitransparent phases

Applying the gray medium approximation is often impossible because of a wide spectral range of the thermal radiation. The optical properties of the same phase can be significantly different at the different wavelengths of the thermal spectrum. For example, it can change from completely opaque to completely transparent. Figure 2 shows that the radiative heat flow can vary by orders of magnitude depending of whether a phase is opaque or transparent. To model porous ceramics with transparent pores and the solid phase transparent in visible and near infrared and opaque in far infrared, consider a heterogeneous medium composed of transparent phase 0 and semitransparent phase 1. The semitransparent phase is absolutely transparent at photon frequencies above the threshold $\nu_{\rm th}$ and absolutely opaque below it. Integral (27) becomes

$$\Lambda = \frac{64 \sigma T^3}{3 \mathcal{A}_{01}} [p H_{\rm inf} + (1 - p) H_{\rm sup}], \tag{50}$$

where

$$p = \int_0^{x_{\rm th}} R dx, \quad x_{\rm th} = \frac{h \nu_{\rm th}}{kT}, \tag{51}$$

$$H_{\rm inf} = \frac{n_0^2 f_0^2}{1 - \rho_{01} R_{01}}, \tag{52}$$

$$H_{\rm sup} = \frac{n_0^2 f_0^2 (1 - \rho_{10} R_{10}) + 2 n_0 n_1 f_0 f_1 T_{01} \sqrt{(1 - \rho_{01})(1 - \rho_{10})} + n_1^2 f_1^2 (1 - \rho_{01} R_{01})}{(1 - \rho_{01} R_{01})(1 - \rho_{10} R_{10}) - T_{01}^2 (1 - \rho_{01})(1 - \rho_{10})}. \tag{53}$$

V. COMPARISON WITH THE MIE THEORY

Let the medium be dilute suspension of polydispersed spheres with the number distribution in diameter $m(D)dD$. Then the specific surface is

$$\mathcal{A}_{01} = \frac{6 f_1}{D_{32}}, \quad \text{with} \quad D_{32} = \frac{\int_0^\infty D^3 m(D) dD}{\int_0^\infty D^2 m(D) dD}, \tag{54}$$

and transport extinction coefficient (38) can be written in the conventional for the Mie theory form[37]

$$\beta_{\rm tr} = \alpha_0 + \frac{3}{2} \frac{f_1}{D_{32}} Q_{\rm tr}, \tag{55}$$

where the transport efficiency of extinction is

$$Q_{\rm tr} = 1 - \rho_{01} R_{01} - \frac{T_{01}^2 (1 - \rho_{01})(1 - \rho_{10})}{1 + \frac{2}{3} \alpha_1 D_{32} - \rho_{10} R_{10}}. \tag{56}$$

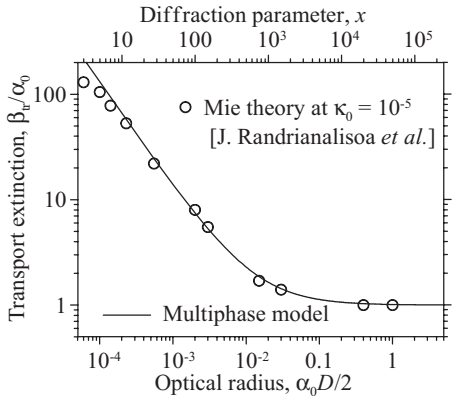

FIG. 3. Normalized transport extinction coefficient β_{tr}/α_0 in fused quartz with 5% bubbles versus the reduced bubble radius $\alpha_0 D/2$: calculated by the Mie theory in Ref. 37 (circles) and estimated by Eq. (55) (line).

Fused quartz with bubbles

Circles in Fig. 3 show the transport extinction coefficient calculated by the theory of Mie in Ref. 37 for a sample of fused quartz containing monodispersed bubbles occupying $f_1=0.05$ of the volume versus the reduced bubble radius $\alpha_0 D/2$. These calculations were made for the refractive index of the quartz matrix $n_0=1.4$ and its extinction index $\kappa_0=\alpha_0\lambda/4\pi=10^{-5}$, where λ is the wavelength. The gas in the bubbles was supposed to be transparent with $\alpha_1=0$ and $n_1=1$. The curve in Fig. 3 shows an estimate by Eq. (55) with the same parameters. The two methods give essentially the same result at the diffraction parameter $x=\pi D/\lambda>10$ (see the upper scale in Fig. 3) while the deviation of geometrical optics-based Eq. (55) from the rigorous Mie theory becomes more and more visible with decreasing x below 10. A considerable discrepancy starts at the diffraction parameter inferior to ~3, meaning that the bubble diameter becomes inferior to the wavelength.

VI. COMPARISON WITH EXPERIMENTS

A. Packed bed of ceramic spheres in vacuum

High-temperature thermal conductivity of packed beds in vacuum reported in Ref. 38 gives the pure radiative conductivity. The conductive component is excluded because the contacts between particles are very small. Figure 4 presents experimental points[38] for ceramic spheres of diameter $D=2.7$ mm packed with the porosity of $f_0=1-f_1=0.42$. The ceramic was Al_2O_3-based with 10% SiO_2 and 1.5% MgO.[38] The long-wavelength absorption edges are about 6 μm for Al_2O_3, 4 μm for SiO_2, and 8 μm for MgO.[39] The lowest value of the transparency threshold $\lambda_{th}=c/\nu_{th}=4$ μm is accepted for the calculation by the model of the mixture of a transparent and a semitransparent phases [Eq. (50)] shown by full line in Fig. 4. The refractive index of particles is taken equal to that of pure Al_2O_3, $n_1=1.7$.[39] The specific surface is estimated by Eq. (54) as $\mathcal{A}_{01}=1289$ m^{-1}.

The maximum of thermal radiation shifts to the visible light with increasing the temperature, where the ceramic particles become more and more transparent. Therefore, at high temperatures the full curve in Fig. 4 approaches to the limit of transparent particles shown by upper broken line. This line is calculated by Eq. (49) with structure factor (53). Inversely, the thermal radiation shifts to the far infrared with decreasing the temperature so that the particles become less transparent and the full curve approaches to the lower broken line corresponding to the limit of opaque particles calculated by Eq. (49) with structure factor (52). The experimental points[38] lie in between the two limits indicating that the semitransparency of the particles is essential in the considered conditions. The model of semitransparent particles given by Eq. (50) satisfactorily describes this experiment.

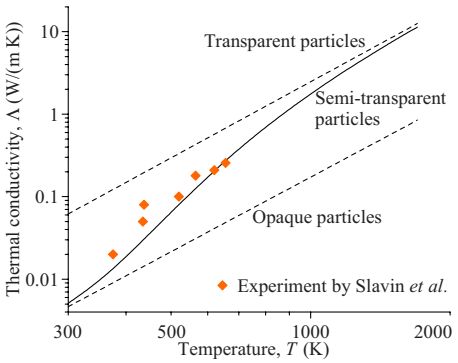

FIG. 4. (Color online) Radiative thermal conductivity Λ of the packed bed of ceramic spheres measured in Ref. 38 as function of temperature T (points) compared with the model of semitransparent particles in transparent matrix according to Eq. (50) (full curve). The broken lines show the gray models of transparent particles (upper broken line) and opaque particles (lower broken line).

B. Packed bed of metallic spheres in air

Thermal conductivity of the packed bed of iron spheres of diameter $D=11$ mm with the porosity of $f_0=1-f_1=0.4$ measured in Ref. 40 is shown in Fig. 5. The pores are filled with air at the atmospheric pressure so that the presented measure-

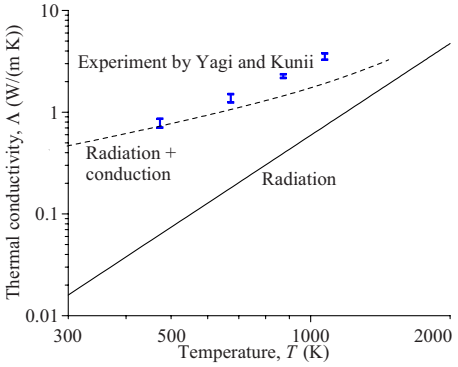

FIG. 5. (Color online) Thermal conductivity of the packed bed of iron spheres in air measured in Ref. 40 as function of temperature T (bars) compared with the model of isotropically scattering opaque particles in transparent matrix according to Eq. (57) (full curve). The broken line gives a correction by thermal conductivity in pores estimated according to Ref. 4.

ments give a superposition of the radiative component and the thermal conductivity through the gas in the pores. The reflectivity of iron strongly depends on the wavelength. However, it is a weak function of the incidence angle except of a very oblique incidence.[36] Therefore, the iron spheres are approximately isotropic scatterers with the vanishing eigenvalue R_{01}. This eliminates the dependence of structure factor (30) on ρ_{01} and proposes a gray model for the radiative conductivity,

$$\Lambda = \frac{64 f_0^2 \sigma T^3}{3\mathcal{A}_{01}}, \tag{57}$$

which is plotted in Fig. 5 by full line. The specific surface $\mathcal{A}_{01}$ is estimated by Eq. (54). A considerable difference between this line and the experimental points proves the importance of heat transfer through the gas phase.

In the considered case of very high ratio of thermal conductivities between the solid and gas phases, the effective thermal conductivity of the packed bed is controlled by pores so that it is proportional to the thermal conductivity of the gas[4] and estimated by the method proposed in Ref. 4 as $17\Lambda_g$ with Λ_g being the thermal conductivity of air. The sum of the radiative and conductive components is shown by broken line in Fig. 5, where the temperature dependence of Λ_g is taken from Ref. 40. The superposition of radiation and conduction still underestimates the experimental data at higher temperatures. This discrepancy can be associated with the natural convection in the pores not taken into account. Note that while the condition of stagnant air is declared in Ref. 40 for the cited experiment, their apparatus with a horizontal temperature gradient cannot exclude the natural convection. In conclusion, the model of radiative conductivity reduced in this case to Eq. (57) is consistent with the experiment of Ref. 40.

C. Packed bed of zirconia microspheres

The dotted line in Fig. 6 shows the best fit[41] $\Lambda = 0.01\ \mathrm{W/(m\ K)} + 1.85 \times 10^{-11}\ \mathrm{W/(m\ K^4)} T^3$ of the measured in Ref. 41 thermal conductivity of a packed bed of hollow yttria-stabilized zirconia microspheres Metco 204B-NS in vacuum. The first term of this fit (the chain line in Fig. 6) is supposed to be the conductivity through small surface contacts between the spheres. The proportionality of the second radiative term to the temperature cubed suggests the gray medium approximation described by Eq. (49). According to the data published in Ref. 42, yttria-stabilized cubic zirconia is transparent at least till 7.5 μm with the refractive index in the near infrared around $n_1 = 2.0$. The structure factor estimated by Eq. (30) is $H = 2.07$ for $\alpha_0 = \alpha_1 = 0$, $n_0 = 1$, $n_1 = 2.0$,[42] and $f_0 = 1 - f_1 = 0.57$.[41] The sphere diameters are in the range from 45 to 75 μm.[41] The size distribution is not reported so that the first approximation to the specific surface is estimated by Eq. (54) with the mean diameter of $D_{32} = 60$ μm corresponding to the middle of this interval. The upper broken line in Fig. 6 shows this estimate to the radiative thermal conductivity, and the upper full line

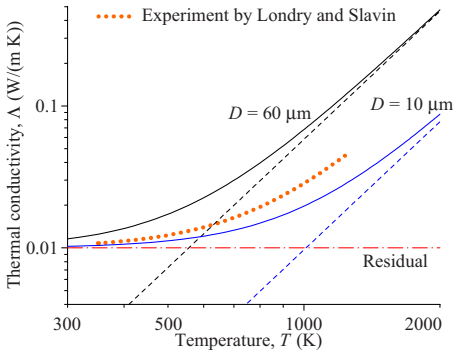

FIG. 6. (Color online) Thermal conductivity Λ of the packed bed of hollow zirconia microspheres in vacuum versus the temperature T: experimental data obtained in Ref. 41 (dotted line); residual conductivity estimated in Ref. 41 (chain line); and theoretical inferior and superior bounds of the radiative (broken lines) and total (full lines) conductivities calculated by the model of transparent spheres of diameter D (marked near the corresponding curves) in transparent matrix.

is the sum of the radiative conductivity with the experimentally measured residual of 0.01 W/(m K) (Ref. 41) due to contact conductivity.

The above theoretical prediction (upper full line in Fig. 6) considerably overestimates the experimental data (dotted line) because of ignoring the internal structure of the hollow microspheres. The radiation can be additionally scattered by phase boundaries inside the microspheres, which decreases the conductivity. Therefore, the upper broken and full lines give superior estimates for the radiative and total thermal conductivity, respectively, in this case. According to the image of the hollow microspheres presented in Ref. 41, they contain smaller spheres with the diameter of about 10 μm. Therefore, the superior estimate of the specific surface is given by Eq. (54) with the mean diameter of $D_{32} = 10$ μm. This corresponds to the inferior estimates of the radiative and total conductivities shown in Fig. 6 by the lower broken and full lines, respectively. The experimental data do lie between the inferior and superior theoretical estimates. However, the two estimates differ by a factor of 6. Such low accuracy of the theoretical calculation is mainly due to insufficient experimental characterization of the morphology of the studied medium, which does not allow precise evaluation of the specific surface.

VII. CONCLUSION

Multiphase radiation transfer model[30] is analyzed by the Chapman-Enskog expansion relevant for optically thick domains. The principal term of this expansion gives Fourier's law for the radiative heat flow. The result of this analysis generalizing the Rosseland diffusion approximation is presented as the radiative thermal conductivity depending on the phase composition of the medium, the specific surface of the phase boundaries, and the spectral optical properties of the phases, namely, the refractive index and the absorption coefficient. It is applicable in the domain of parameters where the scattering of the thermal radiation can be considered in the

approximation of the geometrical optics because the coefficients of the base model[30] are obtained in this approximation. Analytical results are presented for the structural models of dilute dispersed systems with the dispersed particles-isotropic and particles-diffuse scatterers and convex randomly oriented dispersed particles of absolutely opaque and absolutely transparent dielectrics and dense dispersed systems with additional assumptions about the spectral optical properties of the phases. The spectral models of the gray medium and a mixture of a transparent and a semitransparent phases are considered.

The obtained results are compared with the Mie theory for dilute dispersions by considering the example of fused quartz with bubbles.[37] The present model gives essentially the same estimate for the transport extinction coefficient as the Mie theory for the diffraction parameter superior to 10. A considerable deviation from the Mie theory starts at the diffraction parameter inferior to ~3 meaning that the diameter of the dispersed scatterers becomes inferior to the wavelength.

The results are compared with experiments on high-temperature thermal conductivity in packed beds. The model of semitransparent particles given by Eq. (50) satisfactorily describes the thermal conductivity of ceramic spheres in vacuum.[38] The gray medium described by Eq. (49) is expected to be the best model for zirconia microspheres in vacuum.[41] However, the accuracy of the theoretical calculation is low in this case mainly due to insufficient experimental characterization of the morphology of the medium, which does not allow precise evaluation of the specific surface. The analysis of the experimental data on metallic spheres in air[40] is complicated by participation of conduction and, probably, convection in pores. The model of radiative conductivity reduced in this case to Eq. (57) is consistent with this experiment.

*av.gusarov@relcom.ru

[1] J. C. Maxwell, *A Treatise on Electricity and Magnetism* (Dover, New York, 1954).
[2] S. Torquato, *Random Heterogeneous Materials* (Springer, New York, 2002).
[3] M. Rombouts, L. Froyen, A. V. Gusarov, E. H. Bentefour, and C. Glorieux, J. Appl. Phys. **97**, 024905 (2005).
[4] A. V. Gusarov and E. P. Kovalev, Phys. Rev. B **80**, 024202 (2009).
[5] L. Braginsky and V. Shklover, Phys. Rev. B **78**, 224205 (2008).
[6] H. L. Duan and B. L. Karihaloo, Phys. Rev. B **75**, 064206 (2007).
[7] R. Prasher, Phys. Rev. B **74**, 165413 (2006).
[8] E. Stora, Q.-C. He, and B. Bary, J. Appl. Phys. **100**, 084910 (2006).
[9] A. Fiori, I. Jankovic, and G. Dagan, Phys. Rev. Lett. **94**, 224502 (2005).
[10] Y. Jiao, F. H. Stillinger, and S. Torquato, Phys. Rev. E **76**, 031110 (2007).
[11] A. Alzina, E. Toussaint, A. Beakou, and B. Skoczen, Compos. Struct. **74**, 175 (2006).
[12] A. Majumdar, ASME J. Heat Transfer **115**, 7 (1993).
[13] I. Fedina, E. Litovsky, M. Shapiro, and A. Shavit, J. Am. Ceram. Soc. **80**, 2100 (1997).
[14] S. S. Sazhin, E. M. Sazhina, and M. R. Heikal, Fuel **79**, 1843 (2000).
[15] Y. Hua, G. Flamant, J. Lu, and D. Gauthier, Int. J. Heat Mass Transfer **48**, 1145 (2005).
[16] S. Maruyama, H. Nakai, A. Sakurai, and A. Komiya, J. Quant. Spectrosc. Radiat. Transf. **109**, 1 (2008).
[17] A. Abou-Sena, A. Ying, and M. Abdou, Fusion Sci. Technol. **47**, 1094 (2005).
[18] A. S. Sabau, C. E. Duty, R. B. Dinwiddie, M. Nichols, C. A. Blue, and R. D. Ott, J. Appl. Phys. **105**, 084901 (2009).
[19] J. C. Chen and S. W. Churchill, AIChE J. **9**, 35 (1963).
[20] A. J. Slavin, V. Arcas, C. A. Greenhalgh, E. R. Irvine, and D. B. Marshall, Int. J. Heat Mass Transfer **45**, 4151 (2002).
[21] S. Rosseland, *Theoretical Astrophysics* (Oxford University Press, London, 1936).
[22] P. G. Klemens and I. N. Greenberg, J. Appl. Phys. **44**, 2992 (1973).
[23] V. Venugopalan, J. S. You, and B. J. Tromberg, Phys. Rev. E **58**, 2395 (1998).
[24] H. R. Tschudi, Int. J. Heat Mass Transfer **51**, 5008 (2008).
[25] M. I. Mishchenko, L. D. Travis, and A. A. Lacis, *Multiple Scattering of Light by Particles. Radiative Transfer and Coherent Backscattering* (Cambridge University Press, New York, 2006).
[26] D. Baillis and J. F. Sacadura, J. Quant. Spectrosc. Radiat. Transf. **67**, 327 (2000).
[27] J. L. Consalvi, B. Porterie, and J. C. Loraud, Int. J. Heat Mass Transfer **45**, 2755 (2002).
[28] A. V. Gusarov and J.-P. Kruth, Int. J. Heat Mass Transfer **48**, 3423 (2005).
[29] B. Zeghondy, E. Iacona, and J. Taine, Int. J. Heat Mass Transfer **49**, 2810 (2006).
[30] A. V. Gusarov, Phys. Rev. B **77**, 144201 (2008).
[31] W. Lipiński, J. Petrasch, and S. Haussener, J. Quant. Spectrosc. Radiat. Transf. **111**, 253 (2010).
[32] A. V. Gusarov, T. Laoui, L. Froyen, and V. I. Titov, Int. J. Heat Mass Transfer **46**, 1103 (2003).
[33] R. Siegel and J. R. Howell, *Thermal Radiation Heat Transfer* (Taylor & Francis, Washington, 1992).
[34] J. H. Ferziger and H. G. Kaper, *Mathematical Theory of Transport Processes in Gases* (North-Holland, Amsterdam, 1972).
[35] H. C. Van de Hulst, *Light Scattering by Small Particles* (Dover, New York, 1981).
[36] A. V. Gusarov, E. H. Bentefour, M. Rombouts, L. Froyen, C. Glorieux, and J.-P. Kruth, J. Appl. Phys. **99**, 113528 (2006).
[37] J. Randrianalisoa, D. Baillis, and L. Pilon, J. Opt. Soc. Am. A Opt. Image Sci. Vis. **23**, 1645 (2006).
[38] A. J. Slavin, F. A. Londry, and J. Harrison, Int. J. Heat Mass Transfer **43**, 2059 (2000).
[39] D. E. Gray, *American Institute of Physics Handbook* (McGraw-Hill, New York, 1972).
[40] S. Yagi and D. Kunii, AIChE. J. **3**, 373 (1957).
[41] F. A. Londry and A. J. Slavin, J. Am. Ceram. Soc. **74**, 3118 (1991).
[42] D. L. Wood and K. Nassau, Appl. Opt. **21**, 2978 (1982).